energy&fuels

pubs.acs.org/EF Article

Low-Tension Polymer Flooding Using a Short-Hydrophobe Surfactant for Heavy Oil Recovery

Kwang Hoon Baek, Francisco J. Argüelles-Vivas, Gayan A. Abeykoon, Ryosuke Okuno,* and Upali P. Weerasooriya

Cite This: *Energy Fuels* 2020, 34, 15936−15948 Read Online

ACCESS | Metrics & More | Article Recommendations

ABSTRACT: Short-hydrophobe surfactants based on cosolvent species have been studied as novel surfactants for enhanced oil recovery. The objective of this research is to investigate such simple surfactants as a sole additive that enhances the efficiency of oil displacement by creating low-tension polymer (LTP) fronts. This paper presents the potential enhancement of oil displacement efficiency by LTP flooding based on comprehensive experimental data, such as interfacial tensions (IFTs), surfactant partition coefficients, surfactant adsorption in a sandpack, polymer/LTP rheology, and sandpack flooding results. The optimal LTP identified was composed of 0.5 wt % 2-ethylhexanol-7PO-15EO in partially hydrolyzed polyacrylamide polymer solution, which reduced the IFT with heavy oil from 15.8 to 0.025 dyn/cm, without creating microemulsions. The surfactant adsorption in the sandpack was only 0.055 mg-surfactant/g-sand. Sandpack flooding results show that the LTP flooding achieved an incremental oil recovery in comparison to straight-polymer flooding. The oil recovery at 1 pore-volume injected (PVI) was 47% original-oil-in-place (OOIP) for the polymer flooding, 63% for the smaller LTP slugs (0.5 wt % surfactant for 0.1 PVI and 0.1 wt % surfactant for 0.5 PVI), and 70% for the larger LTP slug (0.5 wt % surfactant for 0.5 PVI). Fractional flow theory was applied to confirm that the IFT reduction by 3 orders of magnitude was conducive to a lowered residual oil saturation in LTP flooding, leading to a delayed polymer breakthrough and an increased oil cut thereafter in comparison to polymer flooding.

1. INTRODUCTION

Short alcohols and their alkoxylation forms have been studied as the cosolvent in chemically enhanced oil recovery methods, such as alkali−surfactant−polymer (ASP) flooding.[1−4] Such cosolvent chemicals are used to promote microemulsion phase behavior. For example, Upamali et al. found that the use of alkoxylated short alcohols (isobutyl alcohol, phenol, and 2-ethylhexanol) resulted in microemulsion phase behavior with shorter equilibrium time, smaller microemulsion viscosity, and less surfactant retention.[4]

The objective of this research is to investigate the application of cosolvent-based short-hydrophobe surfactants as a sole additive to polymer solution that moderately lowers the interfacial tension (IFT) between the polymer solution and reservoir oil. Such low-tension polymer (LTP) solution is studied as a slug driven by a straight polymer for displacement of heavy oil in this research.

The improvement in the oil displacement efficiency of polymer flooding was studied by adding surfactants at low concentrations and was referred to as LTP flooding in the 1990s[5,6] before the technological advancements that led to the current practice of SP and ASP flooding, such as new surfactants, their formulations, and salinity gradient. LTP flooding does not use the salinity gradient that is often necessary to use ultralow IFT (10^{-3} dyn/cm) microemulsions in SP and ASP flooding. Since only one chemical is added to polymer solution for LTP flooding, the operation cost is expected to be smaller than in conventional SP and ASP with multiple chemicals. Furthermore, no use of alkali can avoid the potential injectivity issue caused by calcite and silica scales. This research was motivated by a question as to whether the simpler LTP flooding can improve the displacement efficiency of polymer flooding based on the actual field data for a heavy oil reservoir.

LTP flooding may have several advantages particularly for off-shore reservoirs. Off-shore platforms generally have limited space for facilities to handle the large quantities of chemicals. That is, it is more advantageous to use fewer chemicals. Salinity gradient is also more difficult to apply for off-shore reservoirs because either the seawater or the produced water is often the water source for injection. The salinity gradient could be possible when there is a salinity difference between the seawater and the reservoir brine, but the injection of seawater may cause scale precipitation when it is mixed with the reservoir brine.

Recently, short-hydrophobe surfactants were studied by several researchers.[7−9] Wang et al. tested a short-hydrophobe surfactant as a wettability modifier for oil recovery from fractured limestone cores.[7] They found that 2-etheylhexanol-

Received: August 12, 2020
Revised: October 14, 2020
Published: November 23, 2020

https://dx.doi.org/10.1021/acs.energyfuels.0c02720
Energy Fuels 2020, 34, 15936−15948

4PO-15EO (or 2-EH-4PO-15EO) altered the wettability of calcite surfaces from oil-wet (contact angle: 134.1°) to water-wet (contact angle: 47.1°) after 1 day. Then, they conducted dynamic imbibition tests for oil recovery from fractured limestone cores. In comparison to water injection, they achieved 47.3% (OOIP) incremental oil recovery with 1.6 pore volume (PV) of surfactant-brine slug followed by 7.0 PV of brine injection. They demonstrated the potential application of short-hydrophobe surfactants to enhance water imbibition in carbonate reservoirs.

Panthi et al. applied a short-hydrophobe surfactant for heavy oil recovery in a sandpack and sandstones.[8] They used phenol-7PO-15EO as a single additive to the polymer. Both oil and polymer viscosities were approximately 330 cP at 70 °C. Before polymer flooding, water flooding was conducted until there was no more oil production. Then, they injected 0.4 PV of the SP slug followed by 1.5 PV of polymer solution. The final oil recovery was 99.7% (OOIP) for a sandpack, 59.6% (OOIP) for Bentheimer Sandstone, and 31.5% (OOIP) for Berea Sandstone. However, they did not explain the large differences in oil recovery among the different types of porous media. The oil recovery mechanism in their research depended on microemulsion phase behavior as is the case with the conventional SP flooding. In contrast, the current research is concentrated on LTP flooding with no microemulsion for the incremental heavy oil recovery with a short-hydrophobe surfactant.

Baek et al. tested phenol-4PO-20EO for heavy oil recovery in a high-permeability glass-bead pack.[9] They conducted water flooding, 40-cp polymer flooding, and low-tension 40-cp polymer flooding to displace a 276-cp heavy oil. The oil recovery after 2 PV injection was 84% with the LTP flooding, which was 54% and 22% higher than the water flooding and the polymer flooding, respectively. They reduced the IFT from 11 dyn/cm to 0.39 dyn/cm with 2 wt % phenol-4PO-20EO. Their research was limited in that the selection of the optimum surfactant was based on the mixing behavior of surfactant with a heavy oil. This empirical method may not be robust because it relies primarily on visual observation. Also, they conducted an oil displacement experiment with a continuous LTP solution injection, instead of a slug of the LTP solution as typically done in surfactant flooding.

These previous results suggest a potential advantage of LTP flooding using a short-hydrophobe surfactant, especially for heavy oil reservoirs of high permeability. In this research, LTP flooding was tested in oil displacements specifically designed for a heavy oil reservoir, where an economic optimum yielded a polymer viscosity that is substantially smaller than the oil viscosity. Unlike Baek et al.,[9] an optimal short-hydrophobe surfactant was studied by exhaustive IFT measurements because the water−oil IFT is the key to achieving capillary desaturation and delayed the polymer breakthrough in LTP flooding. Also, this paper presents new experimental results of surface adsorption and equilibrium partition coefficients of the short-hydrophobe surfactant used for LTP.

Sections 2 and 3 summarize the materials and the methods used in this research. Section 4 presents the main results from sandpack floods with different injection schemes. Section 5 gives the main conclusions of this research.

2. MATERIALS

The heavy oil sample used in this research has an API gravity of 10.8°. The molecular weight of the heavy oil sample was measured to be 428 g/mol by freezing point depression. The solubility analysis gave the following composition: 53.5 wt % saturates, 22.8 wt % aromatics, 20.8 wt % resins, and 2.9 wt % asphaltenes (*n*-pentane insoluble). The total acid number was 8.08 mg-KOH/g-oil. The dead-oil viscosity was 500 cP at 61 °C, which was the temperature for all sandpack flooding experiments.

The sandpack had a length of 31 cm and a diameter of 2.58 cm. The sandpack was prepared to represent the grain size distribution of the target reservoir. Ottawa sand was filtered into five different grain sizes. Before packing sand, the filtered sand was acidized by 10 wt % HCl solution (2.7 M HCl, pH = −0.44). After the acidizing, each filtered sand sample was refiltered by the same sieve number. The grain size distribution of the sandpack is summarized in Figure 1.

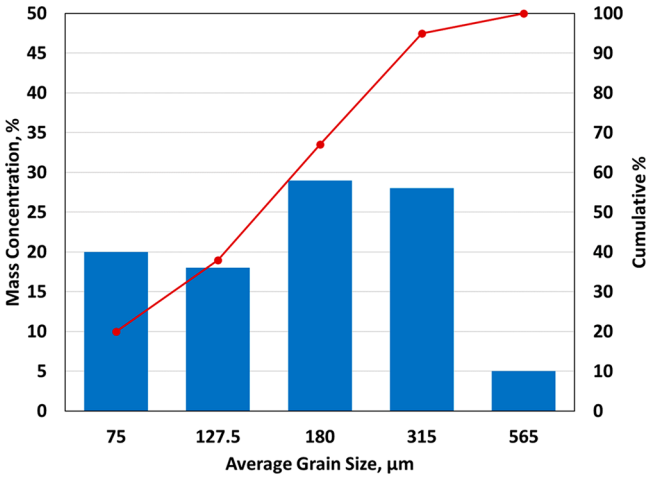

Figure 1. Grain size distribution for the sandpack in this research.

The salinity of the reservoir brine is 56 456 ppm. The produced reservoir brine is expected to be used for polymer flooding in the field. Therefore, the injection brine and the reservoir brine were assumed to be identical as shown in Table 1.

Table 1. Brine Composition

ion	concentration [mg/L]
Na^+	18 387
K^+	200
Ca^{2+}	2015
Mg^{2+}	958
Cl^-	34 883
SO_4^{2-}	13
total dissolved solids	56 456

Short-hydrophobe surfactants were synthesized by the alkoxylation of alcohols: e.g., 2-ethylhexanol (2-EH)-*x*PO-*y*EO or phenol-*x*PO-*y*EO, where *x* is the number of propylene oxide (PO) and *y* is the number of ethylene oxide (EO). The PO and EO groups are related to hydrophobicity and aqueous stability of a surfactant, respectively. A larger number of PO increases the affinity for oil, resulting in a higher level of hydrophobicity. The EO number can be adjusted for the aqueous stability, depending on the brine salinity, brine hardness, and temperature.

In this research, 2-EH-*x*PO-*y*EO and phenol-*x*PO-*y*EO were tested as a short-hydrophobe surfactant to lower the IFT between the polymer solution and heavy oil. Figure 2 shows the chemical structures of these surfactants. A total of 12 surfactants, 2-EH-*x*PO-*y*EO and phenol-*x*PO-*y*EO with different *x* and *y* values, were tested. Table 2 lists the surfactants, all of which were provided by Harcros Chemicals. 2-EH-7PO-15EO has been selected as the optimum surfactant based on IFT measurements as will be discussed in detail in Section 4.

https://dx.doi.org/10.1021/acs.energyfuels.0c02720
Energy Fuels 2020, 34, 15936−15948

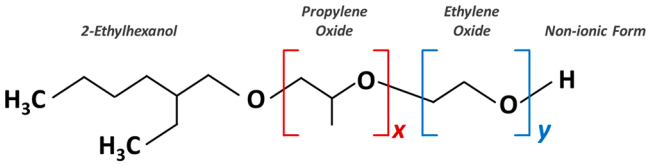

(a) 2-Ethylhexanol-xPO-yEO

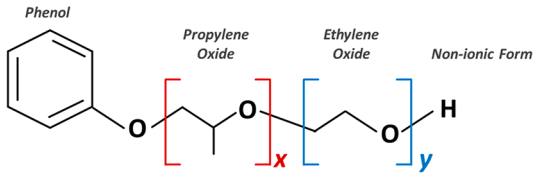

(b) Phenol-xPO-yEO

Figure 2. Chemical structures of the short-hydrophobe surfactants studied in this research.

Table 2. List of the Short-Hydrophobe Surfactants Tested in This Research

2-ethylhexanol		phenol	
-*x*PO	-*y*EO	-*x*PO	-*y*EO
4PO	15	4PO	15
4PO	20	4PO	20
4PO	25	4PO	30
7PO	8	7PO	15
7PO	15	7PO	20
7PO	20	7PO	30

3. METHODS

3.1. Polymer Solution Preparation. Partially hydrolyzed polyacrylamide (HPAM) polymer, Flopaam 3630s (SNF), was used for polymer flooding and LTP flooding. This is a powder-type polymer with an approximate molecular weight of 20 million Dalton.

The polymer concentration was 0.54 wt % in the reservoir brine, which gave the viscosity of approximately 60 cP at a shear rate of 7 s^{-1} at 61 °C, which is much smaller than the viscosity of reservoir oil to be displaced, 500 cP. For LTP flooding, a target concentration of the surfactant was directly added to make LTP.

The polymer solution was prepared while reducing the possibility of any polymer degradation. One batch of polymer solution was no more than 400 mL. The polymer was added after the brine (or brine + surfactant) solutions were prepared. Polymer was added while the solution (brine or brine/surfactant) was under mixing at 500 rpm. Polymer powders should be sprinkled into the solution at the consistent rate manually so that no polymer aggregation occurred.

The mixing of the polymer solution was performed at 500 rpm for 3 h. After mixing, the solution was filtered through a 1.2 μm filter. Filtration ratio (FR) was measured to confirm the homogeneity of the polymer solution. FR was defined as the time (Δt_2) to collect 20 mL from 180 to 200 mL divided by the time (Δt_1) to collect 20 mL from 60 to 80 mL. The polymer solution is acceptable when FR is smaller than 1.2.

$$\text{Filtration Ratio, FR} = \frac{\Delta t_2}{\Delta t_1} = \frac{t_{200\text{mL}} - t_{180\text{mL}}}{t_{80\text{mL}} - t_{60\text{mL}}}$$

After the filtration, the polymer solution was degassed by argon gas for more than 1 h. This was to remove any oxygen in the solution. The prepared polymer solution was used right after degassing when possible. Otherwise, the polymer solution was kept in a refrigerator until its usage.

Figure 3 gives the measured viscosities of the polymer and LTP solutions (0.5 wt % 2-EH-7PO-15EO in the polymer solution) at different shear rates at 61 °C using a rheometer. The effect of the surfactant on the polymer-solution viscosity was not observed.

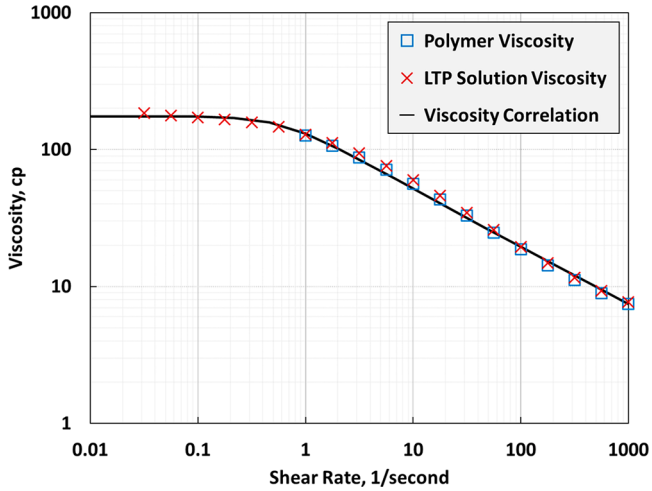

Figure 3. Bulk viscosities of 0.54 wt % HPAM 3630s in the brine (Table 1) with/without the surfactant at 61 °C. The LTP solution contained 0.5 wt % 2-EH-7PO-15EO in the polymer solution.

3.2. In Situ Polymer Viscosity Measurement. Figure 4 shows the experimental setup for in situ viscosity measurement. The system pressure was controlled by ISCO pumps, and the temperature was kept in a Blue M oven at 61 °C. After 3 h of evacuation, the sandpack was filled with brine to measure a porosity. Then, the pressure drops at different brine injection rates were measured to determine a permeability. After determining the porosity and permeability, the polymer solution was injected for more than 1.0 PV to displace the brine completely.

After displacing the brine, the pressure drops at different polymer injection rates were measured to determine the viscosities of the polymer solution at different shear rates. Then, the polymer solution in the sandpack was displaced by the LTP solution. The LTP solution was injected for more than 1.0 PV to displace the polymer solution completely. After displacing the polymer solution, the pressure drops at different LTP injection rates were measured to determine the viscosities of the LTP solution at different shear rates.

3.3. IFT Measurement. A total of 12 short-hydrophobe surfactants were tested, and the water/oil IFT was measured for 11 surfactants after aqueous-stability screening by a spinning drop method (KRÜSS tensiometer) at 61 °C. The surfactant concentration was 1 wt % in the solution at different salinities from zero (i.e., deionized water) to 107 266 ppm. Different salinities were made by dilution or concentration of the reservoir brine (56 456 ppm, Table 1).

3.4. Surfactant Partition Coefficient. Samples were prepared in 20-mL test tubes with five different 2-EH-7PO-15EO concentrations (0.1, 0.2, 0.3, 0.4, and 0.5 wt %) in the reservoir brine. Each sample was prepared with an equal volume (8 mL) between the aqueous and oil phases. Also, samples were prepared with and without polymer in the aqueous phase to observe the effect of polymer on the surfactant partitioning behavior. While samples were aged at 61 °C for 5 days, they were mixed by a vortex mixer 8 times for the first 2 days. Then, samples were aged at room temperature for 5 additional days for equilibration.

Partition coefficients were measured at room temperature because the purpose of this measurement was to assist the analysis of the effluent samples taken at room temperature (see Section 4.5). The concentration of 2-EH-7PO-15EO in the aqueous phase was measured by high-performance liquid chromatography (HPLC). The concentration of 2-EH-7PO-15EO in the oil phase was calculated based on the material balance.

3.5. Tracer Test and Surfactant Adsorption. Figure 4 shows the experimental setup for the tracer test and surfactant adsorption

https://dx.doi.org/10.1021/acs.energyfuels.0c02720
Energy Fuels 2020, 34, 15936−15948

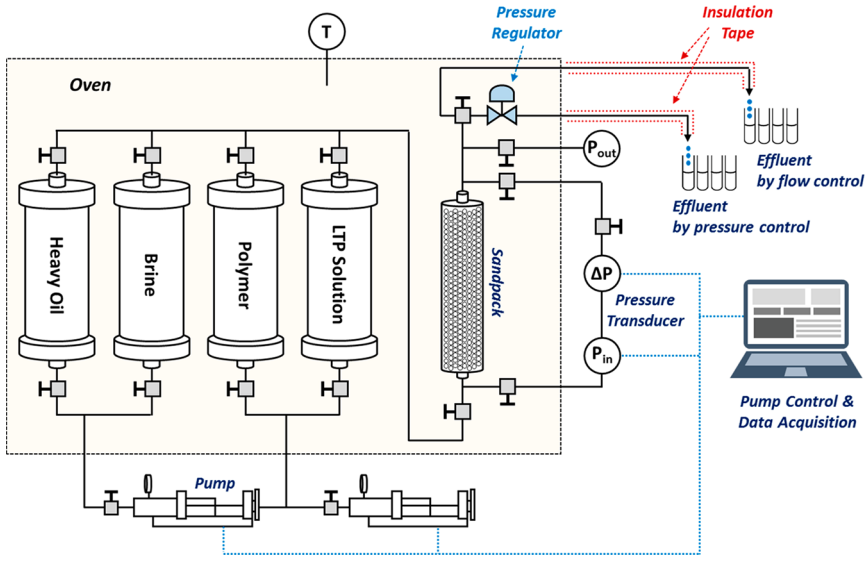

Figure 4. Experimental setup used for the in situ viscosity measurement, tracer test, surfactant adsorption, and sandpack flooding experiment.

Table 3. Summary of the Sandpack Floods in This Research

	straight-polymer flooding	LTP flooding	LTP flooding	LTP flooding
experiment	Flood #1	Flood #2	Flood #3	Flood #4
temperature	61 °C	61 °C	61 °C	61 °C
porous medium	Ottawa sand	Ottawa sand	Ottawa sand	Ottawa sand
porosity	32%	35%	34%	33%
permeability	9.0 Darcy	9.6 Darcy	9.4 Darcy	9.3 Darcy
pore volume	64.7 mL	66.5 mL	66.7 mL	64.4 mL
initial oil saturation	87%	85%	87%	84%
initial water saturation	13%	15%	13%	16%
brine salinity	56 456 ppm	56 456 ppm	56 456 ppm	56 456 ppm
oil viscosity	500 cP	500 cP	500 cP	500 cP
polymer viscosity (at 7 s^{-1})	60 cP	60 cP	60 cP	60 cP
LTP slug	-	0.5 PVI	0.1 PVI	0.5 PVI
		0.1 wt %	0.5 wt %	0.5 wt %
		2-EH-7PO-15EO	2-EH-7PO-15EO	2-EH-7PO-15EO
		0.54 wt %	0.54 wt %	0.54 wt %
		HAPM 3630s	HAPM 3630s	HAPM 3630s
		56 456 ppm	56 456 ppm	56 456 ppm
		brine	brine	brine
polymer injection	5 PVI	4.5 PVI	4.9 PVI	4.5 PVI
	0.54 wt %	0.54 wt %	0.54 wt %	0.54 wt %
	HAPM 3630s	HAPM 3630s	HAPM 3630s	HAPM 3630s
	56 456 ppm	56 456 ppm	56 456 ppm	56 456 ppm
	brine	brine	brine	brine

test. A tracer test was conducted by injecting brine at two different salinities into the sandpack. First, the lower salinity brine with a salinity of 14 114 ppm (4 times lower salinity than the original salinity) was injected for 1.0 PV. Then, the higher salinity brine (the original reservoir brine, Table 1) was injected for 2.0 PV. The pump injection rate was kept at 3 mL/h, corresponding to 1 ft/day. Salinities of effluent samples were measured and matched with the convection−dispersion (CD) equation.

The surface adsorption of 2-EH-7PO-15EO in the sandpack was measured with the compositions of brine, polymer solution, and LTP solution. The procedure of brine saturation in the sandpack was the same as in situ polymer viscosity measurement. After brine saturation, 0.5 PV of the LTP solution was injected, which was followed by 2.5 PV of the polymer solution.

Effluent samples were collected at every 0.05 PV. The concentrations of 2-EH-7PO-15EO in effluent samples were measured by HPLC.

3.6. Sandpack Flooding Experiment. The LTP flooding with a short-hydrophobe surfactant does not expect to have the displacement front of ultralow IFT (i.e., 10^{-3} dyn/cm), which is required for creating the oil bank from dispersed oil droplets after water flooding. Hence, all sandpack flooding experiments were conducted with the initial water saturation at the irreducible saturation; that is, the oil phase was initially present as a continuous phase in the sandpack, and the continuous oil phase was displaced by the polymer or LTP front in this research.

Table 3 gives a summary of the experimental conditions. Straight-polymer flooding was conducted as the baseline of comparison with three LTP floods with different slug properties. The brine salinity was 56 456 ppm for both initial brine and injection solutions (Table 1).

https://dx.doi.org/10.1021/acs.energyfuels.0c02720
Energy Fuels 2020, 34, 15936−15948

No salinity gradient was applied during oil recovery. The total injection volume was 5 PVs for all experiments. The three different LTP cases were (1) 0.5 PV of 0.1 wt % 2-EH-7PO-15EO, (2) 0.1 PV of 0.5 wt % 2-EH-7PO-15EO, and (3) 0.5 PV of 0.5 wt % 2-EH-7PO-15EO, all in 0.54 wt % HPAM 3630s solution. The different slug parameters were tested to see the effect of the 2-EH-7PO-15EO concentration and retention on the final oil recovery.

Figure 4 shows the experimental setup for sandpack flooding. The sandpack and all flow-lines were cleaned and dried at 61 °C for 1 day. After that, the system was evacuated for at least 3 h. Then, the sandpack was saturated with the brine (56 456 ppm). The volume injected indicated the sandpack PV. The brine was injected for several PVs to determine the sandpack permeability using Darcy's equation.

After measuring the porosity and permeability, the heavy oil was injected into the sandpack under a pressure drop of approximately 1 bar to avoid the oversaturation of oil. A total of 200 mL of heavy oil was injected at 10 mL/h for 20 h. Brine was collected from the outlet during the oil injection. Oil breakthrough and water recovery were measured to determine the initial oil and water saturations for the subsequent oil displacement experiment. The end-point relative permeability to oil was estimated after the injection of heavy oil for several PVs.

The injection rate for the straight-polymer flooding (Flood #1) was controlled by the constant pressure drop of 0.44 bar/meter, based on the operation scheme planned for the target reservoir. The outlet pressure was set at 3.45 bar with a back-pressure regulator (BPR). The injection pump was under constant pressure control to keep the pressure drop at 0.44 bar/meter. After the water breakthrough, however, the pump flow rate was fluctuating to keep the constant pump pressure. On average, the injection rate was 1 mL/h until water breakthrough and 3 mL/h after polymer breakthrough to keep the pressure drop of 0.22–0.44 bar/meter.

For LTP floods (Floods #2–#4), the injection rate was controlled by the constant flow rate. The LTP slug was injected at 1 mL/h followed by straight-polymer flooding at 1 mL/h. Then, the polymer injection rate was increased to 3 mL/h after the polymer breakthrough.

4. RESULTS AND DISCUSSION

4.1. In Situ Polymer Viscosity. The bulk phase polymer viscosity measured by a rheometer showed shear-thinning behavior (Figure 3). In many studies of HPAM polymer rheology in porous media, polymer viscosity decreased with increasing shear rate up to a certain point and then increased with further increasing shear rate, which was identified as in situ viscoelastic behavior.[10−17]

Chauveteau tested the in situ viscosity of the HPAM polymer in a glass bead and a sandpack. The concentration of the polymer was between 0.0021 to 0.136 wt %, and the salinity ranged from 2000 to 100 000 ppm total dissolved solids (TDS) (1 to 100 g-NaCl/L). He observed that the viscosity of the HPAM polymer turned from shear-thinning to shear-thickening for all cases.[10] Delshad et al. tested the in situ viscosity of the HPAM polymer (Flopaam 3630s, SNF) in a Berea sandstone. They used 0.15 wt % polymer in 20 000 ppm (TDS) brine. The viscosity of the polymer turned into the shear-thickening behavior when the shear rate was above 20 s^{-1}.[11] Hincapie measured the in situ viscosity of two different HPAM polymers (Hengfloc 63026 and Flopaam 6035s) in a Bentheimer sandstone and a sandpack. He tested 0.05 to 0.15 wt % polymer in 4000 ppm TDS brine. The viscosity behavior of these polymers turned from shear-thinning to shear thickening at shear rates above 20 s^{-1}, as summarized in Rock et al.[13,14] Skauge et al. measured the in situ viscosity of the HPAM polymer (Flopaam 3630s, SNF) in a Bentheimer outcrop. They tested 0.2 wt % polymer in 5000 ppm TDS brine and observed the shear thickening of polymer viscosity at shear rates above 1000 s^{-1}.[15]

Different studies resulted in different rheological characteristics at different shear rates depending on the type of porous media, polymer types and concentrations, and brine compositions and concentrations. Therefore, it is important to measure in situ polymer viscosities before performing the sandpack flooding experiments.

The in situ polymer viscosity depends on in situ shear rate. The in situ shear rate calculation was based on the bundle of tubes model. Hirasaki and Pope provided the in situ shear rate equation derived from the modified Blake–Kozeny model as follows:[18]

$$\dot{\gamma} = \left(\frac{3n+1}{4n}\right)^{n/n-1} \frac{12u}{\sqrt{150k\phi}}$$

where u is the Darcy velocity (superficial velocity), k is the permeability, ϕ is the porosity, and n is the power index from the power-law model of bulk viscosity.

Cannella et al. introduced the correction factor C on the in situ shear rate equation as follows:[19]

$$\dot{\gamma} = C\left(\frac{3n+1}{4n}\right)^{n/n-1} \frac{u}{\sqrt{k\phi}}$$

They tested this model with Berea Sandstone and suggested a value of 6 for the C factor. Experimental data for a sandpack were matched with $C = 4$ in the literature.[20] In this research, therefore, the in situ shear rate equation by Cannella et al. was applied with $C = 4$.

In situ polymer viscosities were calculated by Darcy's equation with the permeability (k), length (L), and cross-sectional area (A) of the porous media and measured pressure drops (ΔP) at different injection rates (q):

$$\mu = \frac{k}{q} A \frac{\Delta P}{L}$$

The absolute permeability of the sandpack was 9.5 Darcy. However, previous studies indicated that the HPAM polymer reduced the permeability of porous media mainly because of polymer adsorption.[17,18,21−25] Therefore, the effective permeability after such a permeability reduction should be considered for in situ viscosity determination. Instead of measuring the effective permeability, it was adjusted with the assumption that in situ polymer viscosity should lie on the bulk-phase polymer viscosity as shown in previous experimental studies.[10,11,13−15] When the absolute permeability (9.5 Darcy) was applied for the in situ shear rate and in situ viscosity, the in situ viscosity was overestimated as shown in Figure 5. The effective permeability was then adjusted to 2.9 Darcy to match the in situ viscosity on the bulk-phase polymer viscosity (Figure 5).

Then, the residual resistance factor (RRF) of the polymer became 3.3 as the ratio between the absolute and effective permeabilities. A RRF value of 3.3 is reasonable for HPAM polymer solution. Wei and Romero-Zerón measured the permeability reduction by the HPAM polymer in a sandpack and RRF as about 3.[26] Skauge et al. measured RRFs of HPAM 3630s in a Bentheimer sandstone. Their measurement results were 3.9 and 7.8 in two different experiments.[15]

Table 4 and Figure 5 summarize the in situ viscosities. The deviation from the shear thinning behavior was observed at

https://dx.doi.org/10.1021/acs.energyfuels.0c02720
Energy Fuels 2020, 34, 15936−15948

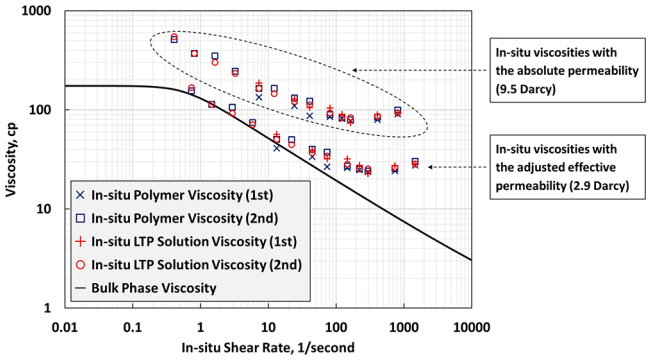

Figure 5. Determination of in situ viscosities for polymer and LTP solutions.

shear rates greater than 10 s^{-1}. This behavior is in line with Rock et al.,[14] who measured in situ HPAM polymer viscosity in a sandpack. As was the case with the bulk viscosities (Figure 2), no difference was observed for the in situ viscosity between the polymer and LTP.

The maximum injection rate of the polymer and LTP solutions in the oil recovery experiments was 3 mL/h that corresponded to an in situ shear rate of 4.4 s^{-1} in this research. Therefore, no deviation from the shear thinning behavior was expected for the polymer solution or the LTP solution during flooding experiments.

4.2. IFT and Critical Micelle Concentration. Table 5 summarizes the IFT data obtained. Results of the IFT measurement show two important trends as shown in Figure 6. First, a lower EO number resulted in a smaller IFT for a given PO number. This confirms the surface activity of the surfactant: propylene oxide (PO) increased the affinity for oil and decreased the IFT, and ethylene oxide (EO) increased the aqueous stability but increased the IFT.

Second, the IFT became smaller with increasing salinity for a given surfactant. As a result, the IFT showed the lowest value near its aqueous stability limit, e.g., 2-EH-7PO-15EO or phenol-7PO-15EO. Therefore, an optimum surfactant was found with the combination of PO and EO numbers that was near the aqueous stability limit and resulted in the smallest IFT, as shown in Figure 7.

2-EH-7PO-15EO was selected as the optimum surfactant based on the IFT data (Figure 6). Then, the CMC was determined for this surfactant by measuring the IFTs at different concentrations in the reservoir brine (Table 1). The same spinning drop tensiometer was used at 61 °C. Table 6 and Figure 8 show that the CMC of 2-EH-7PO-15EO was 0.025 wt % in the reservoir brine and the IFT was stable at 0.025 dyn/cm above the CMC.

Table 5. IFTs Measured for 1 wt % Surfactant Solutions with Heavy Oil at 61 °C.[a]

(a) 2-EH-*x*PO-*y*EO						
	IFT [dyn/cm]					
	2-EH-4PO-			2-EH-7PO-		
salinity [ppm]	15EO	20EO	25EO	8EO	15EO	20EO
0	1.05	4.02	7.40	–	0.27	0.44
5646	0.77	2.45	4.82	–	0.26	0.43
28 228	0.43	0.73	2.32	–	0.094	0.19
56 456*	0.20	0.37	0.87	–	0.025	0.10
84 684	0.088	0.220	0.290	–	–	0.045
107 266	0.040	0.134	0.193	–	–	0.017
(b) Phenol-*x*PO-*y*EO						
	IFT [dyn/cm]					
	phenol-4PO-			phenol-7PO-		
salinity [ppm]	15EO	20EO	30EO	15EO	20EO	30EO
0	11.28	14.89	14.63	1.22	2.77	6.77
5646	6.95	11.25	13.01	1.10	1.71	4.63
28 228	1.81	4.26	8.46	0.68	0.86	2.90
56 456*	1.26	1.80	2.68	0.35	0.49	1.13
84 684	0.91	1.25	1.92	–	0.31	0.65
107 266	–	0.96	1.47	–	0.24	0.49

[a]The asterisk symbol indicates the reservoir brine salinity (Table 1). The "–" sign indicates that the solution was unstable.

Table 4. In Situ Polymer Viscosities Determined Based on the Sandpack Porosity of 0.32, the Sandpack Permeability of 9.5 Darcy with Brine, and the Effective Permeability of 2.9 Darcy with the Polymer and LTP[a]

		in situ viscosity							
		polymer solution				LTP solution			
		first		second		first		second	
injection Rate [mL/h]	in situ shear rate [1/s]	ΔP [bar]	μ [cp]	ΔP [bar]	μ [cp]	ΔP [bar]	μ [cp]	ΔP [bar]	μ [cp]
0.5	0.7			0.038	156.0			0.041	167.4
1	1.5			0.055	113.5			0.055	113.5
2	2.9			0.103	106.4			0.090	92.2
4	5.9			0.145	74.5			0.138	70.9
9	13.2	0.179	41.0	0.221	50.4	0.248	56.7	0.221	50.4
15	22.1			0.365	50.1			0.324	44.4
30	44.1	0.490	33.6	0.586	40.2	0.572	39.2	0.538	36.9
50	73.6	0.648	26.7	0.910	37.5	0.779	32.1	0.834	34.3
100	147.1	1.262	26.0	1.324	27.2	1.551	31.9	1.379	28.4
150	220.7	1.806	24.8	1.848	25.3	2.006	27.5	1.848	25.3
200	294.3	2.310	23.8	2.358	24.3	2.193	22.6	2.468	25.4
500	735.7	5.881	24.2	6.226	25.6	6.633	27.3	6.357	26.2
1000	1471.4	13.445	27.7	14.700	30.2	13.734	28.3	13.852	28.5

[a]For each of the polymers and LTPs, two measurements were performed. Shaded boxes indicate the conditions for which no measurement was done.

https://dx.doi.org/10.1021/acs.energyfuels.0c02720
Energy Fuels 2020, 34, 15936−15948

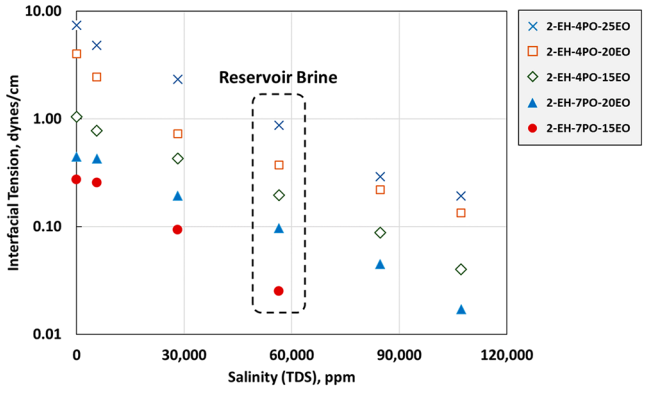

(a) 2-EH-xPO-yEO

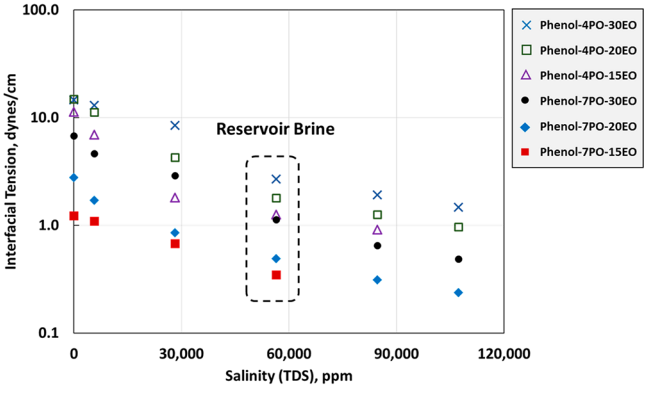

(b) Phenol-xPO-yEO

Figure 6. IFT values measured for 1 wt % 2-EH-*x*PO-*y*EO and phenol-*x*PO-*y*EO with heavy oil at 61 °C.

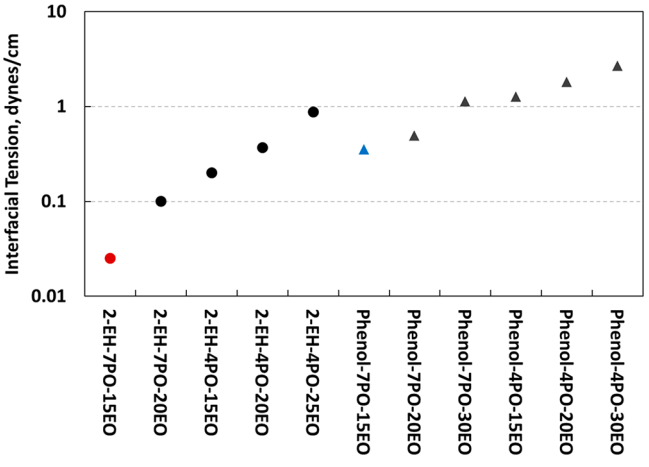

Figure 7. IFT values measure for 1 wt % surfactant in the reservoir brine at 61 °C.

Based on the CMC measurement, the concentration of 2-EH-7PO-15EO was set as 0.5 wt % for LTP to keep the concentration sufficiently above the CMC during sandpack floods considering the inevitable surface adsorption in the sandpack. Note that the total concentration of surfactants in the conventional SP or ASP flooding is usually 1 wt %.[1−3,27,28]

4.3. Partition Coefficient of 2-EH-7PO-15EO between Brine and Oil. Table 7 summarized the partition coefficients of 2-EH-7PO-15EO with different initial surfactant concentrations in the aqueous phase. The results show that the

Table 6. IFT Values Measured for 2-EH-7PO-15EO at Different Concentrations in the Brine (Table 1) with Heavy Oil at 61 °C

2-EH-7PO-15EO concentration in reservoir brine [wt %]	IFT [dyn/cm]
0	15.8
0.0008	6.19
0.0016	5.79
0.0031	3.30
0.0062	1.80
0.013	0.098
0.025	0.025
0.05	0.023
0.1	0.023
0.25	0.023
0.5	0.025
1	0.025

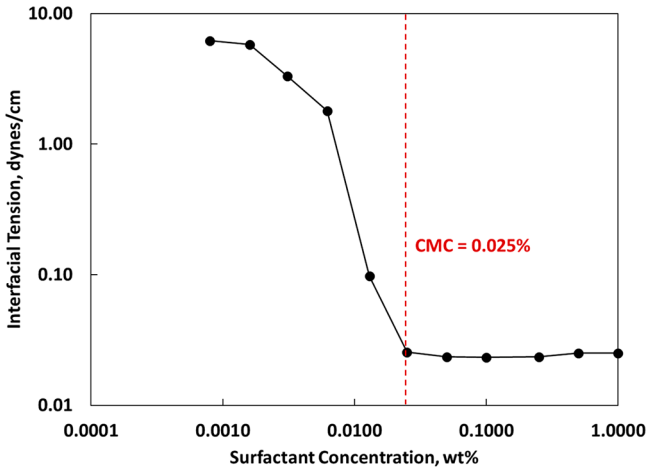

Figure 8. CMC of 2-EH-7PO-15EO in the reservoir brine at 61 °C.

Table 7. Partition Coefficients Measured for 2-EH-7PO-15EO for Heavy Oil and Brine with/without Polymer at Room Temperature[a]

	surfactant concentration after equilibrium			
	aqueous phase		oil phase	
initial surfactant concentration in aqueous phase before mixing [%]	[%]	standard deviation	[%]	partition coefficient
(a) Samples without Polymer				
0.1	0.0201	2.1×10^{-4}	0.0799	3.98
0.2	0.0577	1.4×10^{-3}	0.1423	2.47
0.3	0.0982	8.6×10^{-3}	0.2018	2.05
0.4	0.1570	1.5×10^{-3}	0.2430	1.55
0.5	0.1808	5.5×10^{-3}	0.3192	1.76
(b) Samples with Polymer (0.54 wt % HPAM 3630s)				
0.1	0.0168	7.7×10^{-5}	0.0832	4.97
0.2	0.0548	7.8×10^{-4}	0.1452	2.65
0.3	0.0921	8.2×10^{-4}	0.2079	2.26
0.4	0.1293	1.1×10^{-3}	0.2707	2.09
0.5	0.1920	3.0×10^{-3}	0.3080	1.60

[a]The results are the average values from three repeated measurements. The surfactant concentrations in the aqueous phase were measured, and those in the oil phase were based on the material balance.

https://dx.doi.org/10.1021/acs.energyfuels.0c02720
Energy Fuels 2020, 34, 15936−15948

partition coefficient became larger as the initial surfactant concentration in the aqueous phase decreased. A similar trend was found in the literature. Belhaj et al. measured the partition coefficient of a nonionic surfactant, alkylpolyglucoside.[29] They showed that the partition coefficient decreased with increasing surfactant concentration at surfactant concentrations above the CMC. They explained that, above the CMC, more surfactants remained in the aqueous phase, which decreased the partition coefficient.

Another possible explanation is related to the interaction between divalent cations (e.g., Ca^{2+} and Mg^{2+}) in the aqueous phase and EO groups in the surfactant. Divalent cations are known to deactivate EO groups by chelation. When the 2-EH-7PO-15EO concentration is low, EO groups might not give effective hydrophilicity in the presence of divalent cations. As the EO concentration increases with increased surfactant concentration, the surfactant hydrophilicity can overcome the chelation by divalent cations. Then, a larger amount of the surfactant can stay in the aqueous phase, which reduces the partition coefficient. However, more data on the partition coefficient are required to confirm this explanation.

4.4. Sandpack Properties: Tracer Test and Surfactant Adsorption. The normalized salinities of effluent samples after the tracer test were measured as shown in Figure 9.

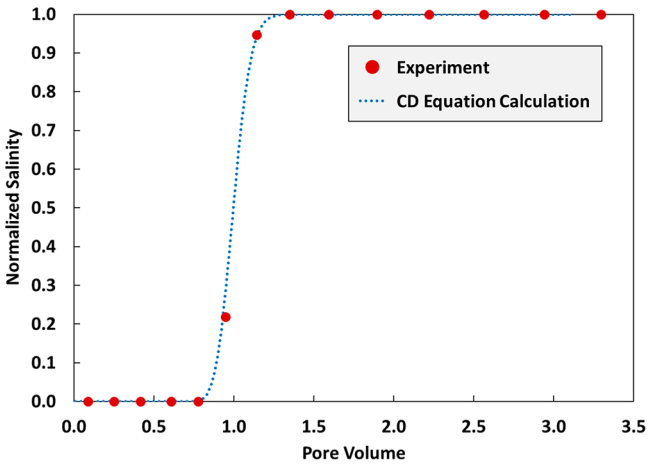

Figure 9. Tracer test results for the sandpack and the matched convection−dispersion (CD) equation solution (porosity: 0.32, length: 31.7 cm, Darcy velocity: 1.3×10^{-4} cm/s, longitudinal dispersion coefficient: 5×10^{-5} cm^2/s, Peclet number: 261).

Hydrodynamic dispersion makes the effluent concentration change smeared. The experimental data were matched with a one-dimensional convection−dispersion (CD) equation. The analytical solution of the CD equation is as follows:[30]

$$C_D = \frac{1}{2}\,\mathrm{erfc}\left(\frac{x_D - t_D}{2\sqrt{\frac{t_D}{N_{Pe}}}}\right) + \frac{e^{x_D N_{Pe}}}{2}\,\mathrm{erfc}\left(\frac{x_D + t_D}{2\sqrt{\frac{t_D}{N_{Pe}}}}\right)$$

The Peclet number (N_{Pe}) is defined as follows:

$$N_{Pe} = \frac{uL}{\phi K_L}$$

where u is the Darcy velocity (cm/s), L is the distance (cm), ϕ is the porosity, and K_L is a longitudinal dispersion coefficient (cm^2/s). In this tracer test, the sandpack porosity (ϕ) was 0.32, the length (L) was 31.7 cm, and the Darcy velocity (u) was 1.3×10^{-4} cm/s. Therefore, experimental data were matched by adjusting a longitudinal dispersion coefficient to 5×10^{-5} cm^2/s. The calculated N_{Pe} was 261. Figure 9 shows the parameters used for the CD equation.

The result of surfactant adsorption is illustrated in Figure 10 with the surfactant concentration in effluent samples. The

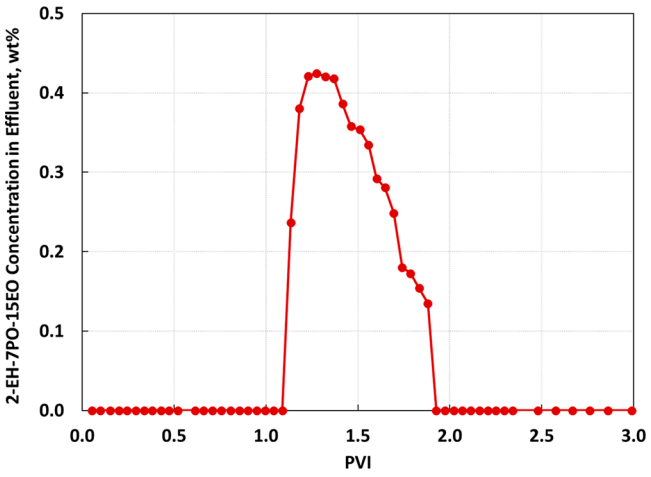

Figure 10. 2-EH-7PO-15EO concentration in effluent samples during surfactant adsorption measurement. A total of 0.178 g of 2-EH-7PO-15EO was injected. The recovered mass from the effluent samples was 0.158 g.

amounts of the injected and recovered mass were 0.178 and 0.158 g, respectively. The difference, 0.020 g, was divided by the mass of the sand particles in the porous medium, 360.5 g, to give the adsorption of 2-EH-7PO-15EO in the sandpack, 0.055 mg-surfactant/g-sand.

4.5. Sandpack Flooding Results. The results of sandpack floods are summarized in Figure 11 (Flood #1), Figure 12

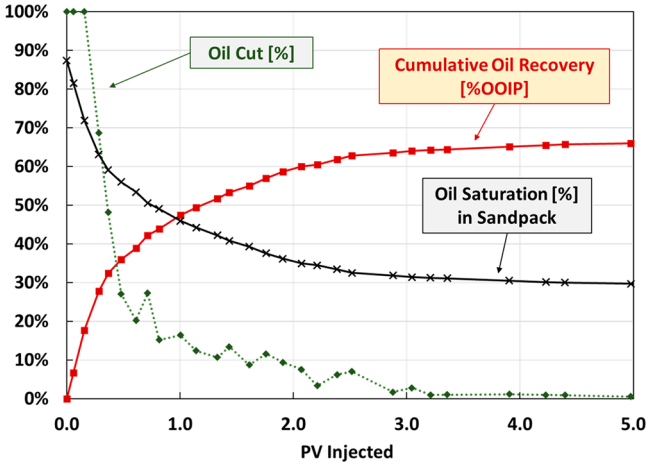

Figure 11. Results for the straight-polymer flooding (Flood #1).

(Flood #2), Figure 13 (Flood #3), and Figure 14 (Flood #4). For the straight-polymer flooding (Flood #1), the water breakthrough occurred before 0.28 PVI. The polymer breakthrough was confirmed at 0.6 PVI based on the oil-cut data. Oil recovery (%OOIP) increased to 47% at 1 PVI, 60% at 2 PVI, and 64% at 3 PVI. The final oil recovery at 5 PVI was 66%. For the LTP flooding (Flood #2) with 0.5 PVI of 0.1 wt

https://dx.doi.org/10.1021/acs.energyfuels.0c02720
Energy Fuels 2020, 34, 15936−15948

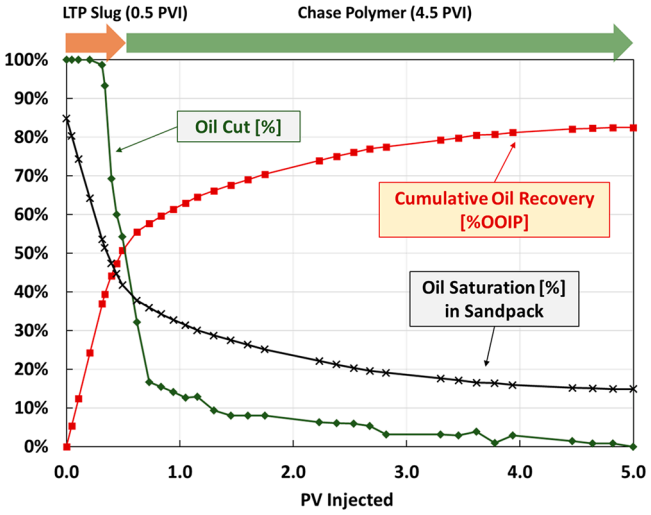

Figure 12. Results for the LTP flooding with 0.5 PV of 0.1 wt % 2-EH-7PO-15EO (Flood #2).

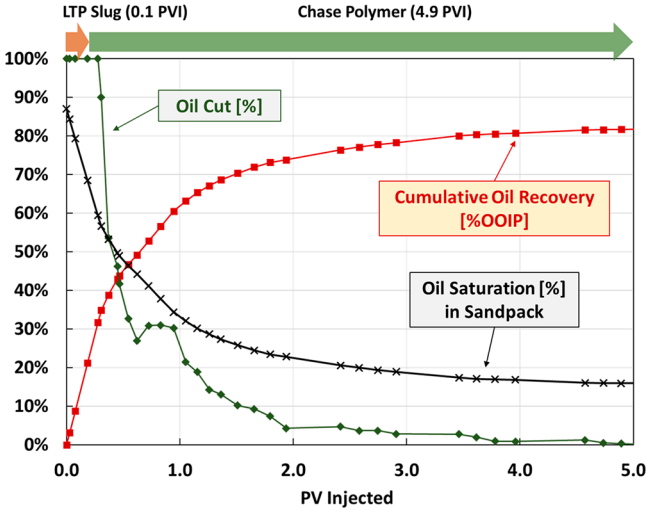

Figure 13. Results of the LTP flooding with 0.1 PV of 0.5 wt % 2-EH-7PO-15EO (Flood #3).

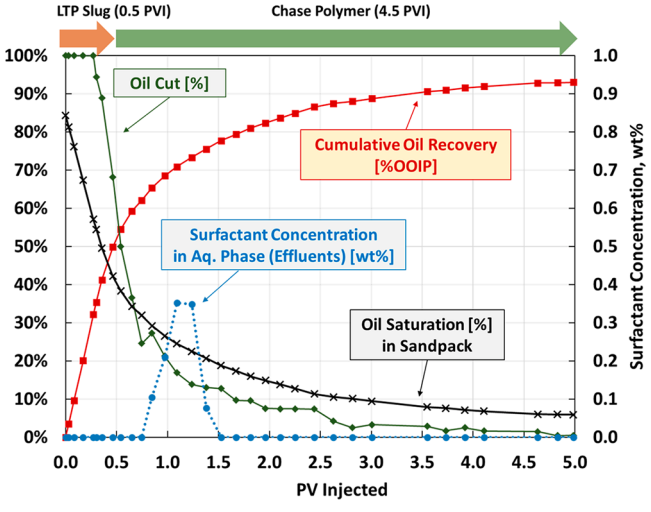

Figure 14. Results of the LTP flooding with 0.5 PV of 0.5 wt % 2-EH-7PO-15EO (Flood #4).

% surfactant, the water breakthrough occurred before 0.31 PVI. Based on the oil cut, the polymer breakthrough was confirmed at 0.73 PVI. The oil recovery (%OOIP) increased to 63% at 1 PVI, 72% at 2 PVI, and 78% at 3 PVI. The final oil recovery at 5 PVI was 82%. For the LTP flooding (Flood #3) with 0.1 PVI of 0.5 wt % surfactant, the water breakthrough occurred before 0.31 PVI. Based on the oil cut, the polymer breakthrough was confirmed at 0.72 PVI. The oil recovery (%OOIP) increased to 63% at 1 PVI, 74% at 2 PVI, and 78% at 3 PVI. The final oil recovery at 5 PVI was 82%. For the LTP flooding (Flood #4) with 0.5 PVI of 0.5 wt % surfactant, the water breakthrough occurred before 0.3 PVI. Based on oil cut, the polymer breakthrough was confirmed at 0.75 PVI. The oil recovery (% OOIP) increased to 70% at 1 PVI, 82% at 2 PVI, and 89% at 3 PVI. The final oil recovery at 5 PVI was 93%.

Only 47% of the total injected 2-EH-7PO-15EO was measured in the aqueous phase of the effluent samples for Flood #4 (Figure 12). No 2-EH-7PO-15EO was detected in the effluent samples for Floods #2 and #3. A large fraction of 2-EH-7PO-15EO might have resided in the sandpack after the experiment. If we assume the surface adsorption of 0.020 g (Section 4.2) and the partition coefficient of 1.60 for the effluent samples (Table 7b), the surfactant distribution after Flood #4 is estimated as follows: 47% for the effluent water, 15% for the effluent oil, 12% in the surface adsorption, and 26% in the water and oil phases in the sandpack. Although this estimation is based on various assumptions, it indicates the potential importance of controlling the partitioning behavior of the surfactant for designing LTP flooding even if the surface adsorption is small.

Table 8 and Figure 15 compare four sandpack floods. They clearly show that the LTP flooding achieved an incremental oil

Table 8. Summary of Oil Recovery Data from the Four Floods (They Are Compared in Figure 15)

	oil recovery [%OOIP]			
PVI	Flood #1	Flood #2	Flood #3	Flood #4
0.5	36	51	45	51
1.0	47	63	63	70
1.5	54	68	70	78
2.0	60	72	74	82
2.5	63	76	76	87
3.0	64	78	78	89
3.5	64	80	80	91
4.0	65	81	81	92
4.5	66	82	82	93
5.0	66	82	82	93

recovery in comparison to the straight-polymer flooding. At 1 PVI, the incremental oil recovery by LTP was 16% for Floods #2 and #3, and 23% for Flood #4. At 2 PVI, the incremental oil recovery became 12%, 14%, and 22% for Floods #1, #2, and #3, respectively. At 5 PVI, the final incremental oil recovery was 16% for Floods #2 and #3 and 27% for Flood #4. After 1 PVI until 5 PVI, the LTP flooding achieved the incremental oil recovery of about 12−16% for Floods #2 and #3 and 22−27% for Flood #4.

The main reason for the incremental oil recovery was the delayed polymer breakthrough. The water breakthrough times for all experiments were similar to each other (approximately at 0.3 PVI). After the water breakthrough, however, the oil cuts for the LTP floods were higher until the polymer break-

https://dx.doi.org/10.1021/acs.energyfuels.0c02720
Energy Fuels 2020, 34, 15936−15948

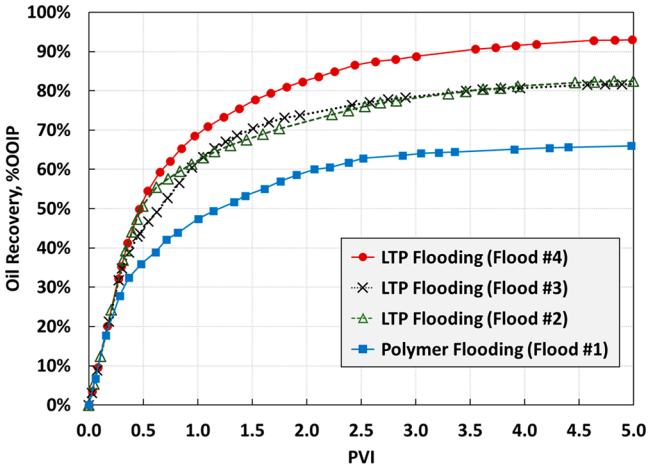

Figure 15. Comparison of oil recovery results among Floods #1−4 (see Table 3 for the experimental conditions). Numerical values for this figure are given in Table 8.

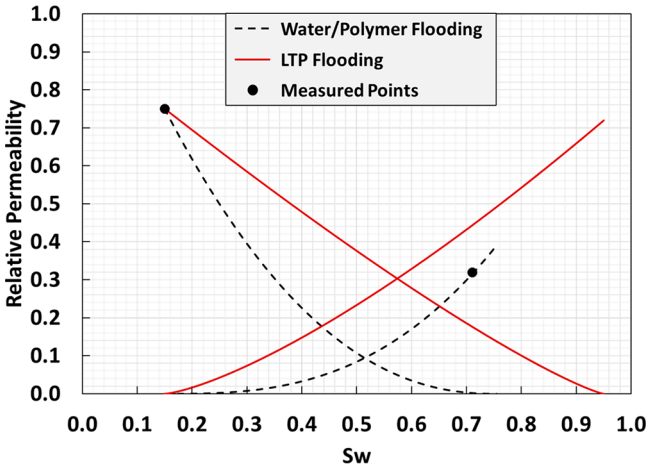

Figure 16. Relative permeability curves determined by matching the sandpack flooding data. Residual water saturations: 0.15 for water/polymer/LTP flooding. Residual oil saturations: 0.245 for water/polymer flooding and 0.05 for LTP flooding. End-point relative permeability of water: 0.39 for water/polymer flooding and 0.72 for LTP flooding. End-point relative permeability of oil: 0.75 for water/polymer flooding and LTP flooding. Exponent for water: 2.8 for water/polymer flooding and 1.36 for LTP flooding. Exponent for oil: 2.25 for water/polymer flooding and 1.2 for LTP flooding.

through. Flood #4 showed the most delayed polymer breakthrough, and the oil cut after the polymer breakthrough was higher than those in Floods #2 and #3.

The delayed polymer breakthrough and higher oil cuts indicate that 2-EH-7PO-15EO increased the oil fractional flow by reducing the IFT between the displaced and displacing fluids. Note that the IFT between the heavy oil and the reservoir brine was 15.8 dyn/cm, and it was reduced to 0.025 dyn/cm with 2-EH-7PO-15EO (Table 6). Using 9.5 Darcy for the permeability, 30.48 cm for the length, and 0.44 bar/meter for the pressure drop, the capillary numbers are calculated to be 2.7×10^{-5} for the straight-polymer flood and 1.7×10^{-2} for the LTP floods. A reduction in the residual oil (or remaining oil) saturation was possible by capillary desaturation at the capillary number increased by 3 orders of magnitude.

The same amount of 2-EH-7PO-15EO was injected for Floods #2 and #3. They compare different slug injection schemes between the smaller concentration with the larger PVI (Flood #2) and the larger concentration with the smaller PVI (Flood #3). They showed slightly different oil recoveries until 2.5 PVI. Flood #2 showed a larger oil bank right after the water breakthrough with a smaller oil cut later; Flood #3 showed a smaller oil bank right after the water breakthrough with a larger oil cut until 2.5 PVI. After 2.5 PVI, the oil recoveries were nearly the same for both cases. A greater oil recovery at the early stage of PVI is important in terms of the economic feasibility of LTP flooding. It seems to be important to study the effect of the surfactant partitioning on the oil displacement efficiency by LTP because Table 7 indicated that the partition coefficient is sensitive to the overall concentration of the surfactant.

4.6. Fractional Flow Calculation. Fractional flow theory was applied to the results of Flood #1 (straight-polymer flooding) and Flood #4 (0.5 PVI of 0.5 wt % LTP). In addition to the basic assumptions of fractional flow, it was assumed that the initial water saturation was at the residual saturation. Figure 16 shows the relative permeability curves adjusted to match the experimental data, especially the polymer breakthrough time of Flood #4 and the final oil recovery of Floods #1 and #4.

For fluid properties, the measured viscosities of brine (0.7 cP) and oil (500 cP) were applied. The viscosity of the polymer and LTP solutions was assumed to be 100 cP, which corresponds to the in situ polymer viscosity at the shear rate of 2 s^{-1}. Since the polymer viscosity was not constant during sandpack flooding, this assumption would not be accurate for matching the fractional flow with the experimental results. A polymer retention was calculated from experimental data from the literature. Zhang and Seright measured the retention of the HPAM polymer (SNF, Flopaam 3230s) in a sandpack. Polymer retention increased from 4.63 to 27.8 μg/g-sand as the polymer concentration increased from 20 to 2000 ppm.[31] Based on these data, the polymer retention of 0.54 wt % HPAM 3630s was calculated as 66 μg/g for both the polymer flooding and the LTP flooding.

Figure 17 shows the fractional flow and the oil recovery results. The fractional flow calculation matched Flood #4 better than Flood #1 likely because the unstable pressure drop control caused the polymer viscosity to fluctuate for Flood #1. Except for the oil recovery around the polymer breakthrough, however, the fractional flow calculation gave a good agreement with the experimental data. According to the matched relative permeabilities, the residual oil saturation was reduced from 24.5% to 5% for Flood #4. This indicates that the capillary number during the LTP flooding increased to cause a significant reduction of the residual oil saturation.

The LTP flooding has the potential of improving the heavy-oil displacement by polymer especially when straight-polymer flooding is not quite effective under an adverse mobility ratio. The LTP flooding can increase oil recovery by delaying the polymer breakthrough and increasing the oil cut thereafter as shown by the experimental data and the matched fractional flow.

5. CONCLUSIONS

LTP flooding was tested with a cosolvent-based short-hydrophobe surfactant, 2-EH-7PO-15EO, as a sole additive to the polymer solution in terms of the displacement efficiency of heavy oil in a sandpack. The experimental conditions were set based on the field data available for an actual heavy oil reservoir, in which no salinity gradient and alkali injection were

https://dx.doi.org/10.1021/acs.energyfuels.0c02720
Energy Fuels 2020, 34, 15936−15948

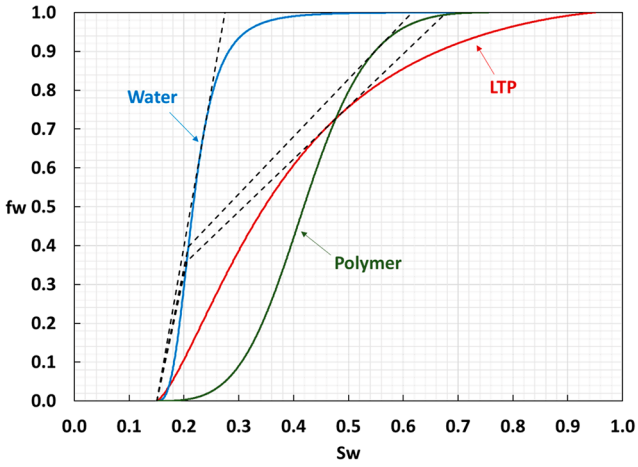

(a) Fractional Flow

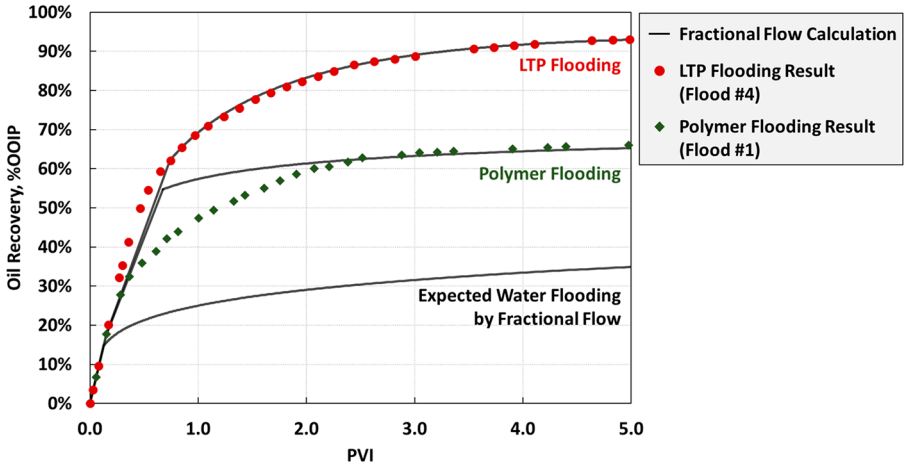

(b) Oil Recovery (%OOIP)

Figure 17. Fractional flow construction and oil recovery histories from the fractional flow theory and experimental data.

considered. Three LTP floods were performed with different slug sizes and concentrations and compared with straight-polymer flooding. The key conclusions are as follows:

1. The optimal surfactant was selected through IFT measurements in this research. Each short-hydrophobe surfactant gave the lowest IFT near its solubility limit. 2-EH-7PO-15EO was selected as the optimum surfactant with the lowest IFT among the 12 surfactants tested. The IFT between the heavy oil and the aqueous solution was 0.025 dyn/cm at 61 °C. The CMC of 2-EH-7PO-15EO was 0.025 wt % in the reservoir brine at 61 °C.
2. The surfactant adsorption of 2-EH-7PO-15EO was 0.055 mg-surfactant/g-rock in the sandpack, which is substantially smaller than the typical values reported for ionic surfactants in the conventional SP. The small adsorption is desirable for effective use of the injected surfactant for sweeping/displacing heavy oil.
3. The LTP flooding (Floods #2, #3, and #4) achieved an incremental oil recovery in comparison to the straight-polymer flooding (Flood #1). The oil recovery (% OOIP) at 1 PVI was 47% for Flood #1, 63% for Floods #2 and #3, and 70% for Flood #4. After 1 PVI until 5 PVI, the LTP flooding achieved the incremental oil recovery of 12−16% for Floods #2 and #3 and 22−27% for Flood #4.
4. The optimal LTP reduced the IFT by 3 orders of magnitude as demonstrated in this research. However, it is unlikely to make an oil bank from dispersed oil droplets in the continuous water phase after water flooding, which often requires more complex surfactant formulations for ultralow IFT (i.e., 10^{-3} dyn/cm). In this research, therefore, the LTP flooding was tested for an actual field case, in which a continuous oil phase in the reservoir is expected, but straight-polymer flooding is adversely affected by a large mobility of the polymer solution. In comparison to the polymer flooding, the LTP flooding increased the oil recovery with the delayed polymer breakthrough and the higher oil cut after the breakthrough.

AUTHOR INFORMATION

Corresponding Author

Ryosuke Okuno − *Hildebrand Department of Petroleum and Geosystems Engineering, The University of Texas at Austin,*

https://dx.doi.org/10.1021/acs.energyfuels.0c02720
Energy Fuels 2020, 34, 15936−15948

Austin, Texas 78712, United States; orcid.org/0000-0003-3675-1132; Email: okuno@utexas.edu

Authors

Kwang Hoon Baek − *Hildebrand Department of Petroleum and Geosystems Engineering, The University of Texas at Austin, Austin, Texas 78712, United States*

Francisco J. Argüelles-Vivas − *Hildebrand Department of Petroleum and Geosystems Engineering, The University of Texas at Austin, Austin, Texas 78712, United States*

Gayan A. Abeykoon − *Hildebrand Department of Petroleum and Geosystems Engineering, The University of Texas at Austin, Austin, Texas 78712, United States*

Upali P. Weerasooriya − *Hildebrand Department of Petroleum and Geosystems Engineering, The University of Texas at Austin, Austin, Texas 78712, United States*

Complete contact information is available at: https://pubs.acs.org/10.1021/acs.energyfuels.0c02720

Notes

The authors declare no competing financial interest.

■ ACKNOWLEDGMENTS

We gratefully acknowledge the financial support from JX Nippon Oil & Gas Exploration Corporation and the Chemical EOR Industrial Affiliates Project at the University of Texas at Austin. Ryosuke Okuno holds the Pioneer Corporation Faculty Fellowship in Petroleum Engineering at The University of Texas at Austin. The authors thank Dr. Kishore K. Mohanty for sharing their lab equipment for this research.

■ REFERENCES

(1) Aitkulov, A.; Luo, H.; Lu, J.; Mohanty, K. K. Alkali-Cosolvent-Polymer Flooding for Viscous Oil Recovery: 2D Evaluation. *Energy Fuels* **2017**, *31*, 7015−7025.

(2) Fortenberry, R.; Kim, D.; Nizamidin, N.; Adkins, S.; Arachchilage, G.; Koh, H. S.; Weerasooriya, U. P.; Pope, G. A. Use of Cosolvents to Improve Alkaline/Polymer Flooding. *SPE Journal* **2015**, *20*, 255−266.

(3) Sharma, H.; Panthi, K.; Mohanty, K. K. Surfactant-Less Alkali-Cosolvent-Polymer Floods for an Acidic Crude Oil. *Fuel* **2018**, *215*, 484−491.

(4) Upamali, K. A. N.; Liyanage, P. J.; Jang, S. H.; Shook, E.; Weerasooriya, U. P.; Pope, G. A. New Surfactants and Cosolvents Increase Oil Recovery and Reduce Cost. *SPE Journal* **2018**, *23*, 2202−2217.

(5) Kalpakci, B.; Arf, T. G.; Barker, J. W.; Krupa, A. S.; Morgan, J. C.; Neira, R. D. The Low-Tension Polymer Flood Approach to Cost-Effective Chemical EOR. *Proceedings of the SPE/DOE Enhanced Oil Recovery Symposium*, 22−25 April 1990, Tulsa, OK, U.S.A.; Society of Petroleum Engineers: 1990; SPE-20220-MS, DOI: 10.2118/20220-MS.

(6) Maldal, T.; Gilje, E.; Kristensen, R.; Karstad, T.; Nordbotten, A.; Schilling, B. E. R.; Vikane, O. Evaluation and Economical Feasibility of Polymer-Assisted Surfactant Flooding for the Gullfaks Field, Norway. *SPE Reservoir Evaluation & Engineering* **1998**, *1*, 161−168.

(7) Wang, M.; Baek, K.; Abeykoon, G. A.; Argüelles-Vivas, F. J.; Okuno, R. A Comparative Study of Ketone and Surfactant for Enhancement of Water Imbibition in Fractured Porous Media. *Energy Fuels* **2020**, *34*, 5159−5167.

(8) Panthi, K.; Weerasooriya, U. P.; Mohanty, K. K. Chemical Flood of a Viscous Oil with Novel Surfactants. *Proceedings of the SPE Annual Technical Conference and Exhibition*, 30 September−2 October 2019, Calgary, Alberta, Canada; Society of Petroleum Engineers: 2019; SPE-196198-MS, DOI: 10.218/196198-MS.

(9) Baek, K.; Argüelles-Vivas, F. J.; Abeykoon, G. A.; Okuno, R.; Weerasooriya, U. P. Application of Ultrashort Hydrophobe Surfactants with Cosolvent Characters for Heavy Oil Recovery. *Energy Fuels* **2019**, *33*, 8241−8249.

(10) Chauveteau, G. Molecular Interpretation of Several Different Properties of Flow of Coiled Polymer Solutions Through Porous Media in Oil Recovery Conditions. *Proceedings of the SPE Annual Technical Conference and Exhibition*, 4−7 October 1981, San Antonio, TX, U.S.A.; Society of Petroleum Engineers: 1981; SPE-10060-MS, DOI: 10.2118/10060-MS.

(11) Delshad, M.; Kim, D. H.; Magbagbeola, O. A.; Huh, C.; Pope, G. A.; Tarahhom, F. Mechanistic Interpretation and Utilization of Viscoelastic Behavior of Polymer Solutions for Improved Polymer-Flood Efficiency. *Proceedings of the SPE Symposium on Improved Oil Recovery*, 20−23 April 2008; Tulsa, OK, U.S.A.; Society of Petroleum Engineers: 2008; SPE-113620-MS, DOI: 10.2118/113620-MS.

(12) Han, X.; Wang, W.; Xu, Y. The Viscoelastic Behavior of HPAM Solutions in Porous Media and It's Effects on Displacement Efficiency. *Proceedings of the International Meeting on Petroleum Engineering*, 14−17 November 1995, Beijing, China; Society of Petroleum Engineers: 1995; SPE-30013-MS, DOI: 10.2118/30013-MS.

(13) Hincapie, R. E. Pore-Scale Investigation of the Viscoelastic Phenomenon during Enhanced Oil Recovery (EOR) Polymer Flooding through Porous Media. Ph.D. Dissertation, The Clausthal University of Technology, 2016; ISBN: 978-3-86948-531-7.

(14) Rock, A.; Hincapie, R. E.; Wegner, J.; Ganzer, L. Advanced Flow Behavior Characterization of Enhanced Oil Recovery Polymers using Glass-Silicon-Glass Micromodels that Resemble Porous Media. *Proceedings of the SPE Europec featured at 79th EAGE Conference and Exhibition*, 12−15 June 2017, Paris, France; Society of Petroleum Engineers: 2017; SPE-185814-MS, DOI: 10.2118/185814-MS.

(15) Skauge, T.; Skauge, A.; Salmo, I. C.; Ormehau, P. A.; Al-Azr, N.; Wassing, L.; Glasbergen, G.; Van Wunnik, J. N.; Masalmeh, S. K. Radial and Linear Polymer Flow - Influence on Injectivity. *Proceedings of the SPE Improved Oil Recovery Conference*, 11−13 April 2016, Tulsa, OK, U.S.A.; Society of Petroleum Engineers: 2016; SPE-179694-MS, DOI: 10.2118/179694-MS.

(16) Skauge, A.; Zamani, N.; Gausdal Jacobsen, J.; Shaker Shiran, B.; Al-Shakry, B.; Skauge, T. Polymer Flow in Porous Media: Relevance to Enhanced Oil Recovery. *Colloids Interfaces* **2018**, *2*, 27.

(17) Sorbie, K. S. *Polymer-Improved Oil Recovery*; Springer Netherlands: 1991; ISBN 978-0-216-92693-6.

(18) Hirasaki, G. J.; Pope, G. A. Analysis of Factors Influencing Mobility and Adsorption in the Flow of Polymer Solution Through Porous Media. *SPEJ, Soc. Pet. Eng. J.* **1974**, *14*, 337−346.

(19) Cannella, W. J.; Huh, C.; Seright, R. S. Prediction of Xanthan Rheology in Porous Media. *Proceedings of the SPE Annual Technical Conference and Exhibition*, 2−5 October 1988, Houston, TX, U.S.A.; Society of Petroleum Engineers: 1988; SPE-18089-MS, DOI: 10.2118/18089-MS.

(20) Koh, H.; Lee, V. B.; Pope, G. A. Experimental Investigation of the Effect of Polymers on Residual Oil Saturation. *SPE Journal* **2018**, *23* (1), 001−017.

(21) Gogarty, W. B. Mobility Control With Polymer Solutions. *SPEJ, Soc. Pet. Eng. J.* **1967**, *7*, 161−173.

(22) Mishra, S.; Bera, A.; Mandal, A. Effect of Polymer Adsorption on Permeability Reduction in Enhanced Oil Recovery. *J. Pet. Eng.* **2014**, *2014*, 1−9.

(23) Smith, F. W. 1970. The Behavior of Partially Hydrolyzed Polyacrylamide Solutions in Porous Media. *JPT, J. Pet. Technol.* **1970**, *22*, 148−156.

(24) White, J. L.; Goddard, J. E.; Phillips, H. M. Use of Polymers To Control Water Production in Oil Wells. *JPT, J. Pet. Technol.* **1973**, *25*, 143−150.

(25) Zaitoun, A.; Chauveteau, G. Effect of Pore Structure and Residual Oil on Polymer Bridging Adsorption. *Proceedings of the SPE/DOE Improved Oil Recovery Symposium*, 19−22 April 1998, Tulsa, OK,

U.S.A.; Society of Petroleum Engineers: 1998; SPE-39674-MS, DOI: 10.2118/39674-MS.
(26) Wei, B.; Romero-Zerón, L. The Evaluation of a Technological Trend in Polymer Flooding for Heavy Oil Recovery. *Pet. Sci. Technol.* **2014**, *32*, 2396−2404.
(27) Sharma, H.; Dufour, S.; Arachchilage, G. W. P. P.; Weerasooriya, U. P.; Pope, G. A.; Mohanty, K. K. Alternative alkalis for ASP flooding in anhydrite containing oil reservoirs. *Fuel* **2015**, *140*, 407−420.
(28) Tagavifar, M.; Herath, S.; Weerasooriya, U. P.; Sepehrnoori, K.; Pope, G. A. Measurement of Microemulsion Viscosity and Its Implications for Chemical Enhanced Oil Recovery. *SPE Journal* **2018**, *23*, 066−083.
(29) Belhaj, A. F.; Elraies, K. A.; Alnarabiji, M. S.; Shuhli, J. A. B. M.; Mahmood, S. M.; Ern, L. W. Experimental Investigation of Surfactant Partitioning in Pre-CMC and Post-CMC Regimes for Enhanced Oil Recovery Application. *Energies* **2019**, *12*, 2319.
(30) Lake, L. W.; Johns, R.; Rossen, B.; Pope, G. *Fundamentals of Enhanced Oil Recovery*; Society of Petroleum Engineers: 2014; ISBN: 978-1-61399-328-6.
(31) Zhang, G.; Seright, R. Effect of Concentration on HPAM Retention in Porous Media. *SPE Journal* **2014**, *19*, 373−380.

https://dx.doi.org/10.1021/acs.energyfuels.0c02720
Energy Fuels 2020, 34, 15936−15948